

Can black carbon in snow be detected by remote sensing?

Stephen G. Warren¹

Received 11 July 2012; revised 29 November 2012; accepted 30 November 2012; published 30 January 2013.

[1] In remote areas of the Northern Hemisphere, typical mixing ratios of black carbon (BC) in snow are 3–30 ng/g. In cold fine-grained snow these BC amounts can reduce the broadband albedo by 0–1% and the visible-wavelength albedo by 0–2%, representing significant climatic forcings. In melting snow the reductions are larger, 0–3% and 1–6%, respectively. Surface albedos inferred from satellite measurements have typical errors of a few percent, so a signal of reduced albedo will be difficult to detect. The inference of albedo from a nadir radiance measurement can be biased low because of undetected thin clouds or blowing snow altering the angular reflectance pattern. But even if the albedo could be measured perfectly from satellite, its attribution would be ambiguous because of the vertical variation of snow grain size, absorbing aerosol in the atmosphere above the snow, and especially because of subpixel heterogeneity of the thin and patchy snow cover of the Arctic and many other treeless regions. The spectral signature of thin snow resembles that of BC in snow. For these reasons, attempts to use satellite remote sensing to estimate the BC content of snow, or the reduction of albedo by BC, are unlikely to be successful, except in highly polluted industrial regions.

Citation: Warren, S. G. (2013), Can black carbon in snow be detected by remote sensing?, *J. Geophys. Res. Atmos.*, 118, 779–786, doi:10.1029/2012JD018476.

1. Introduction

[2] Recent interest in black carbon (BC) in snow as an agent for radiative forcing of climate, inspired by the climate modeling work of *Hansen and Nazarenko* [2004], has motivated studies of the optical properties of carbonaceous particles, methods of BC measurement, Arctic air pollution, measurements of BC mixing ratio in snow, and radiative transfer modeling of this forcing and its climatic effects.

[3] Measurement of BC in snow has been done using three methods: (1) filtration followed by spectrophotometry [Clarke and Noone, 1985], (2) the thermo-optical method [e.g., Forsström et al., 2009], and (3) the single-particle soot photometer (SP2) [e.g., McConnell et al., 2007]. Our own work has used method (1): melting snow samples of mass 200–2000 grams and filtering the meltwater [Doherty et al., 2010; Huang et al., 2010], then measuring the filters in a spectrophotometer [Grenfell et al., 2011]. The fieldwork to collect the samples is time consuming, and in the large regions of interest, such as Russia, Canada, or the Arctic Ocean, it is practical to sample only a small number of widely spaced sites. It is therefore appropriate to ask whether the reduction of snow albedo could be detected from radiance measurements by satellite or unmanned aerial vehicles

(UAVs), and whether such measurements could distinguish the effect of BC from other influences on snow albedo. In recent years I have been invited to join proposals that promised to achieve these objectives for Arctic snow. I have declined those invitations because I think such efforts are destined to fail; this paper explains why.

[4] Median values for the BC content (C_{BC}) of Arctic snow range from 3 ppb on the Greenland Ice Sheet to 34 ppb in northeast Siberia [Doherty et al., 2010]. (The abbreviation “ppb” here means parts per 10^9 by mass, equivalent to nanograms of BC per gram of snow.) For a typical snow grain size in springtime, prior to the onset of melt (radiatively effective radius $r_e = 100 \mu\text{m}$), these BC amounts can reduce broadband snow albedo by 0–1%, and visible albedo by 0–2% [Warren and Wiscombe, 1985, Figure 2]. For old melting snow with coarser grains, $r_e = 1 \text{ mm}$, the reductions are 0–3% and 1–6%, respectively. (New computations, using updated optical constants of ice and updated optical properties of BC, some of which are shown in Figure 1, are actually in close agreement with the 1985 results.) For a typical daily average solar irradiance of 400 W m^{-2} in the Arctic late spring and early summer, a 1% reduction of broadband albedo causes a positive forcing of 4 W m^{-2} locally. Because of the large efficacy of this forcing agent [Hansen et al., 2005; Flanner et al., 2007], such a seemingly small albedo change translates into a significant climatic forcing. Here I outline the difficulties of using remote sensing to determine snow albedo to this accuracy, and the difficulties of attributing a measured albedo reduction to a specific cause. The paper discusses remote-sensing considerations mainly for the Arctic and the Northern Hemisphere midlatitudes, because that is where a significant radiative forcing can be expected; in the Antarctic the levels of BC and other light-absorbing

¹Department of Atmospheric Sciences, University of Washington, Seattle, Washington, USA.

Corresponding author: S. G. Warren, Department of Atmospheric Sciences, University of Washington, Box 351640, Seattle, WA 98195–1640, USA. (sgw@uw.edu)

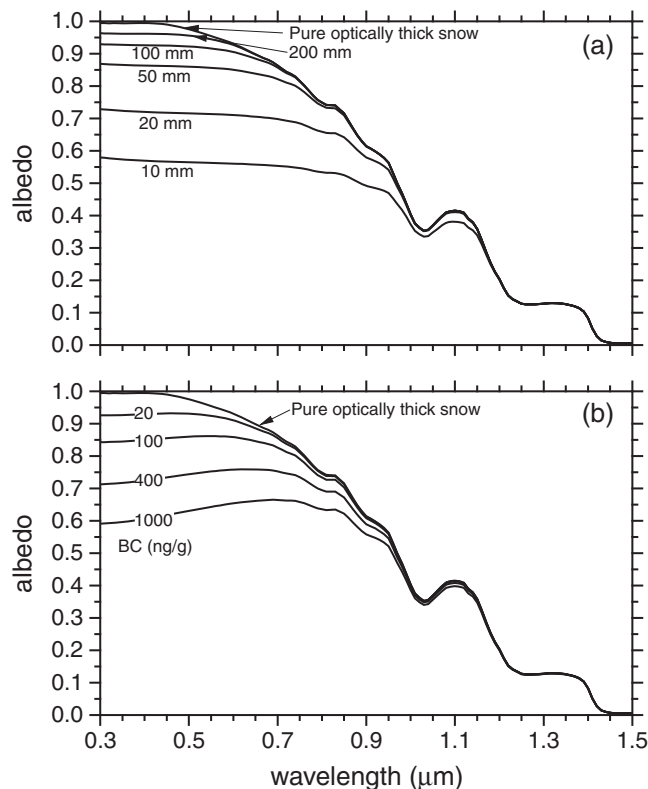


Figure 1. Comparison of the spectral signature of snow thinness to that of black carbon (BC) in snow, for snow grain radius $r_e = 1$ mm and solar zenith angle $\theta_0 = 60^\circ$. (a) Spectral albedo of pure snow over a black surface for a variety of snow depths expressed in liquid equivalent. The top curve is for semi-infinite depth. Redrawn from Figure 13c of *Wiscombe and Warren* [1980], using updated optical constants of ice [*Warren and Brandt*, 2008]. (b) Spectral albedo of deep snow containing various mixing ratios of BC in parts per billion by mass (nanograms of BC per gram of snow). Redrawn from Figure 7b of *Warren and Wiscombe* [1980], using updated optical constants of ice and BC. The optical constants and size distribution for BC used in the model are those described by *Brandt et al.* [2011]. The digital values for this figure are available at http://www.atmos.washington.edu/ice_optical_constants.

impurities (LAI) are far too low to affect the albedo [*Warren and Clarke*, 1990; *Grenfell et al.*, 1994].

2. Factors Affecting Snow Albedo

[5] Snow albedo varies dramatically with wavelength λ . The albedo is very high at ultraviolet and visible wavelengths, ~ 0.99 for pure snow at $\lambda = 500$ nm [*Wiscombe and Warren*, 1980; *Grenfell et al.*, 1994], but much lower in the near infrared (NIR), $\lambda > 1000$ nm, because of vibrational absorption bands of the water molecule. The NIR albedo is sensitive to the snow grain size; in coarse-grained snow the photon paths through ice are longer so there is a greater probability of absorption. It is the area-to-mass ratio (specific surface area, SSA [e.g., *Matzl and Schneebeli*, 2006, 2010]) that determines the photon survival probability. The SSA can be converted to an effective radius r_e [e.g., *Grenfell and Warren*, 1999]:

$$\text{SSA} = 3/(r_e \rho_{\text{ice}}), \quad (1)$$

where ρ_{ice} is the density of pure ice, 917 kg m^{-3} .

[6] The NIR albedo is also sensitive to solar elevation: at low sun a photon's first scattering event occurs closer to the surface so it is more likely to escape. Cloud cover can affect the spectral albedo by altering the angular distribution

of incident sunlight. The albedo at visible wavelengths is insensitive to solar elevation because the albedo is nearly 1.0 even for high sun, so it cannot increase with zenith angle.

[7] The albedo of pure deep snow at visible and ultraviolet wavelengths (300–700 nm) is insensitive to grain size and solar elevation but is instead sensitive to absorptive impurities such as BC, and to snow depth if the snowpack is thinner than ~ 1 m (Figure 1). In the NIR these two variables have little effect because ice is more absorptive there, with the consequences that (1) small amounts of impurities cannot compete with ice for absorption, and (2) the light penetrates only a short distance into snow, so that even thin snowpacks of only a few centimeters are optically semi-infinite [*Warren and Wiscombe*, 1980]. If the snowpack is thin or contains absorptive impurities, its visible albedo becomes sensitive additionally to snow grain size, because sunlight penetrates deeper in coarse-grained snow than in fine-grained snow [*Warren and Wiscombe*, 1980, Figure 7; *Warren*, 1982, Table 2; *Twohy et al.*, 1989, Figure 1].

[8] A suggested procedure for remote sensing of BC in snow would be as follows:

- (1) Identify cloud-free scenes. This is difficult over snow but is often possible.

- (2) Choose two channels in the visible and two in the NIR. Take the ratio of the reflectances in the NIR channels to estimate the effective grain size (a weighted average for the near-surface snow, over a depth determined by the choice of wavelengths) [e.g., *Nolin and Dozier*, 2000].
- (3) Use the visible channels to obtain the reduction of albedo by absorptive impurities. Together with the grain-size estimate, the albedo reduction will imply an impurity content if the contributions of different impurity types can be distinguished. The ratio of the two visible reflectances would be used to distinguish BC (a grey absorber) from mineral dust and brown carbon (which are less absorptive at red than at blue wavelengths), with uncertainty due to uncertainty in the spectral mass absorption cross-sections (MACs) of dust and brown carbon [*Doherty et al.*, 2010, and references therein].

[9] More channels than these four could be used to improve accuracy but are unlikely to yield qualitatively different information, because of the smooth wavelength-variation of radiative properties of condensed matter (as opposed to gases) [e.g., *Barrow*, 1962, Figure 7.1].

3. Albedo Measurement or Inference

[10] The albedo is the cosine-weighted integral of the radiance over all directions in the upward hemisphere, divided by the incident flux. Satellite instruments use a narrow field of view ($nfov$), so they measure the upward radiance into a particular direction, and additional information is then needed to convert that radiance into an albedo. Because a UAV flies closer to the surface, it can carry a wide-field-of-view ($wfov$) instrument, collecting radiation from the entire hemisphere without an excessively large “footprint.” Some sources of error affect only $nfov$ instruments, and some affect both $nfov$ and $wfov$ instruments (Table 1). Some errors are specific to $wfov$ instruments, in particular the tilt of the detector plane away from horizontal under a clear sky, and deviations from cosine-response. The deviations from cosine-response are wavelength dependent, but their effects are complex because of the wavelength-dependence of the diffuse/direct ratio [*Grenfell et al.*, 1994, Figures 2, 3, and 8]. These topics are discussed by *Grenfell* [2011]. *Grenfell et al.* [1994, Figure 9] shows that the albedo error for snow at visible wavelengths caused by a 2-degree surface slope with solar zenith angle $\theta_o = 70^\circ$ was 5–10%. A comparable error would be caused by a tilted instrument over a horizontal surface, but in this case most of the error would be caused by inaccuracy in the downward flux rather than the upward flux. If the downward flux can be corrected, the error is just 2% (the third factor in equation (4) of *Grenfell et al.* [1994]).

[11] The manufacturers of commercial broadband and narrowband flux instruments (pyranometers) commonly used for albedo measurements from UAVs typically claim radiometric accuracy of 5 W m^{-2} or 5–10%. Some users of these instruments have estimated smaller errors, 1–2% in flux by *Greuell et al.* [2002] for broadband pyranometers and 4% in albedo by *Stroeve et al.* [2001] for a near-visible band (0.4–1.1 μm).

[12] *Greuell and Oerlemans* [2005] measured visible-channel albedos over the Greenland Ice Sheet from a

helicopter, and compared them with albedos reported from simultaneous satellite overpasses of the Moderate Resolution Imaging Spectroradiometer (MODIS) at the same wavelengths (MODIS channels 1, 2, and 4). Their Table 4 shows that the average surface albedos for snow inferred from MODIS were lower than those measured by helicopter, by 0.01–0.03. These values are the average biases; individual values shown in their Figure 7 exhibit larger deviations.

[13] Albedo measurements from satellites and UAVs may become more accurate in the future. Spectral radiometers offer higher accuracy than broadband pyranometers. However, even the best measurements of spectral albedo made at the snow surface do not claim accuracy better than 0.01 [*Brandt et al.*, 2011; *Grenfell et al.*, 1994], and even that accuracy can be obtained only under diffuse lighting (overcast cloud), which minimizes the effects of detector tilt and effects of deviations from cosine response.

4. Anisotropic Reflectance of Snow

[14] A narrow-field-of-view instrument on a satellite will measure the radiance into a particular direction, which can be converted into an albedo if the anisotropic reflectance factor (ARF) [*Suttles et al.*, 1988] is known. The ARF varies with wavelength. For example, comparing two wavelength bands commonly used for satellite remote sensing, over Antarctic snow at $\theta_o = 69^\circ$ the forward peak (viewing zenith angle $\theta_v = 82.5^\circ$) at $\lambda = 600 \text{ nm}$ is twice the angular-average brightness but at $\lambda = 1600 \text{ nm}$ it is five times the average brightness [*Hudson et al.*, 2006, Figure 5]. This variation with wavelength itself depends on grain size, and also on snow depth if the snowpack is thin. The presence of BC in the snow will also alter its visible ARF (relatively more forward scattering, less scattering to zenith), because the penetration depth of light is less when the snow contains BC. An iterative procedure would therefore be needed to infer albedo (iterating steps 2 and 3 of section 2).

[15] The ARF is particularly sensitive to surface roughness. Surface roughness occurs at many scales and with various shapes on snow: ripples, sastrugi [*Gow*, 1965; *Armstrong et al.*, 1973] and suncups [*Post and LaChapelle*, 2000; *Rhodes et al.*, 1987]. Sastrugi are wind-erosion features, resembling longitudinal dunes. On sea ice there are also pressure ridges [*Armstrong et al.*, 1973], which are much larger. The effect of sastrugi on the ARF has been measured [*Warren et al.*, 1998] and modeled [*O’Rawe*, 1991; *Leroux and Fily*, 1998]. The height and direction of sastrugi are altered after each strong windstorm, and their height-to-width ratios are unpredictable. The effects of sastrugi on ARF are different at the different wavelengths, because they depend on the ratio of sastrugi width to flux-penetration depth (which varies with wavelength); the effects are moderated if photons entering one side of a sastruga can survive to escape from the opposite side [*Warren et al.*, 1998, section 8]. Measurements were made at the South Pole, which may be typical of the Antarctic Plateau. At $\lambda = 900 \text{ nm}$ and $\theta_o = 67^\circ$, the radiance in the forward direction, relative to the angular-average brightness, was 2.8 for the solar azimuth aligned with the sastrugi, compared to 2.0 for the solar azimuth perpendicular to the sastrugi [*Warren et al.*, 1998, Figure 5].

[16] The major effects of sastrugi on ARF are at large viewing zenith angles [Warren *et al.*, 1998; Masonis and Warren, 2001]. Warren *et al.* [1998] showed that if remote sensing is restricted to $\theta_v < 50^\circ$, the errors in inferred albedo due to lack of knowledge of sastrugi dimensions and orientations could be limited to 8%. Near-nadir measurements will be the least affected; 2–3% error for the Sun at $\theta_o = 67^\circ$ [Warren *et al.*, 1998, Figure 6a].

[17] In addition to redistributing the reflected radiation with angle, sastrugi can also reduce the albedo by altering the incidence angle of the sunlight and by “trapping,” as reviewed by Warren *et al.* [1998, section 8]. Both Kuhn [1974] and Carroll and Fitch [1981] measured broadband shortwave albedo at the South Pole to be greater by 2% for parallel Sun than for perpendicular Sun. These effects are for the high plateau where the winds are weak so the sastrugi height-to-width ratio is only ~ 0.1 [Warren *et al.*, 1998, Table 2].

[18] Even without significant sastrugi, the ARF can be affected by snow-grain shapes, as shown by Hudson and Warren [2007, Figure 13] for the case of surface frost.

5. Thin Clouds and Blowing Snow

[19] Over snow surfaces, thin low clouds and thin layers of near-surface atmospheric ice crystals (“diamond dust”) are particularly difficult to detect from satellite. A thin

Table 1a. Sources of Error in Direct Measurement of Albedo From Wide-Field-of-View (wfov) Instruments on UAVs and Inference of Albedo From Narrow-Field-of-View (nfov) Measurements on Satellites or UAVs

	wfov	nfov
Tilt of detector plane	+	-
Deviations from cosine response of detector	+	-
Sastrugi effect on anisotropic reflectance factor (ARF)	-	+
Grain-shape effect on ARF	-	+
Nadir reflectance reduced by cloud, fog, diamond dust, or blowing snow	-	+

Table 1b. Sources of Error in Attribution of Albedo Reduction, but Not in Absolute Albedo^a

	wfov	nfov
Reduction of albedo by “trapping” in sastrugi fields	+	+
Grain size increasing with depth	+	+
Thin snow masquerading as BC	+	+
Arctic haze below the instrument	+	+

^aA plus sign refers to measurement that is affected by this source of error.

ground-fog (or diamond-dust layer) can partially hide the surface roughness; measurements by Hudson and Warren [2007, hereafter HW] show that in this case the forward peak is enhanced and the nadir view is darker, even though the

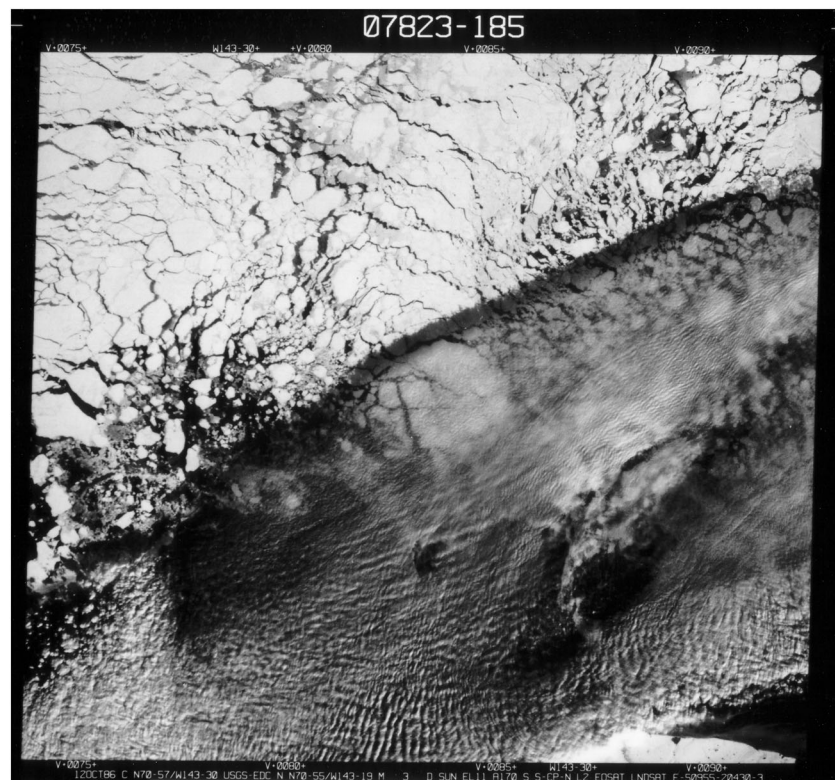


Figure 2. Landsat scene of partial cloud cover over snow-covered sea ice in the Beaufort Sea, 71°N, 144°W, 12 October 1986 [Welch and Wielicki, 1989]. The solar elevation is 11°, and the Sun is shining from the bottom right of the frame (southeast). The upper part of the image is cloud-free. The shadow of the cloud is apparent as the dark band extending from bottom left to top right. The width of the frame is 185 km; spatial resolution is 57 m. (From Figure 1 of Hudson and Warren [2007].)

albedo is probably unchanged or slightly higher. Blowing snow has a similar effect. Analysis of satellite data over Antarctica from the Multiangle Imaging Spectroradiometer (MISR) showed that for $\theta_o = 61^\circ$, clouds of optical depth $\tau \approx 10$ caused a reduction of the nadir brightness by 7%, compensating for a brightening of the forward peak (at $\theta_v = 70^\circ$) by 35% (HW, Figure 11). On the Antarctic Plateau, measurements from atop a 32-m tower, looking down onto a thin ground-fog ($\tau \approx 0.05$) showed that the fog reduced the nadir brightness by 4.5%, more than half what the thicker clouds seen by MISR were able to do (data interpolated from Figure 8 of HW by Stephen Hudson, personal communication, 2011).

[20] The darkening at nadir caused by an undetected cloud could be mistaken for soot-contamination. Figure 2 illustrates this darkening effect of clouds over snow, in a nadir view from Landsat over the Arctic Ocean.

6. Snow Thinness Masquerading as BC

[21] The topics discussed so far dealt with errors in inference of surface albedo, summarized in Table 1a. Next we consider cases where even if the albedo is determined accurately, the attribution of an albedo reduction is ambiguous (Table 1b).

[22] Figure 1 shows that the spectral signature of thin pure snow over a dark underlying surface resembles that of deep sooty snow, in that the albedo is reduced in the visible wavelengths but not in the near infrared. The albedo of BC-laden snow may increase slightly with wavelength from 0.3 to 0.9 μm as shown in Figure 1b, or may instead be flat or decrease slightly, depending on the size distribution of the BC [Brandt *et al.*, 2011, Figures 2 and 4].

[23] Figure 1a shows that even with 200 mm liquid-water equivalent, corresponding to 60 cm of snow with density 300 kg m^{-3} , the pure-snow albedo at $\lambda = 400 \text{ nm}$ for 1 mm grain radius is still 3% below its asymptotic value. Because of their similar spectral signatures, the BC content cannot be determined from satellite radiance measurements unless the snow thickness is independently known. Many attempts have been made to use microwave emission to infer snow depth, but they have been unsuccessful, probably because of the multitude of factors affecting microwave emission by snow [Warren, 1982, Table 2]. Snow depth on Arctic sea ice averages only $\sim 30 \text{ cm}$ ($\sim 110 \text{ mm}$ of liquid equivalent) during May, the month of maximum snow depth [Warren *et al.*, 1999]. Furthermore, the thickness varies over horizontal scales of meters because of wind drifting, so the Arctic snow is often patchy (Figure 3). Even for 30 cm thickness the Arctic tundra vegetation can poke up through the snow, causing albedo reduction that could erroneously be attributed to BC. On the Arctic Ocean, the underlying sea-ice surface may have moderately high albedo, but snow thinness is still significant in reducing the albedo relative to deep snow [Warren and Wiscombe, 1980, Figure 8]. Of probably greater importance in the Arctic Ocean is albedo reduction by sub-grid-scale leads of open water or new dark snow-free ice, which could likewise be erroneously attributed to BC.

[24] A similar situation, but even more extreme, exists on the Tibetan Plateau, a region whose snowpack pollution has received attention from modelers [e.g., Qian *et al.*, 2011]. Over the Tibetan Plateau the snow cover is thin and patchy. On a trip through the northern part of the Tibetan Plateau in February, Huang *et al.* [2011] were able to find snow for sampling of impurities only at mountain passes; they estimated that the fractional area of snow cover in the region was only 1–2%. Flanner and Zender [2005, Figure 3b] show that in



Figure 3. Thin and patchy snow cover on rocky tundra south of Tiksi in northeast Siberia, near the coast of the Arctic Ocean (72°N , 129°E), in early April 2008, about one month before the time of maximum snow depth. (Figure 13 of Doherty *et al.* [2010].)

February, the time of maximum snow depth, the average snow depth in Tibet is only 2 cm, corresponding to about 8 mm liquid equivalent. Remotely sensed signals will therefore include not only the effects of impurities but also the reductions in albedo due to absorption of sunlight by the underlying land surface.

7. Grain Size Increasing With Depth

[25] The snow grain size usually increases with time as "destructive metamorphism" [LaChapelle, 1969] reduces the surface-to-mass ratio (SSA). On the other hand, "constructive metamorphism" can cause growth of depth hoar, whose SSA may be either larger or smaller than the grains from which it metamorphosed. The effective grain radius r_e therefore commonly increases with depth, but often not monotonically. Relative to a homogeneous snowpack, an increase of grain size with depth (within limits) will cause a greater decrease in visible albedo than in NIR albedo because of the greater penetration depth of the visible light [Warren, 1982, section F2]. In a remote-sensing measurement this spectral pattern could be misinterpreted as a signal of BC contamination.

[26] Both snow grain size and BC content vary vertically within the snowpack because individual snowfall events bring different levels of impurities, and because snow grain size evolves with time depending on the temperature history of the snowpack. Such vertically resolved information can be obtained from in situ measurements but would be difficult to infer from remote sensing even if a complete high-resolution spectrum of wavelengths is available.

8. Arctic Haze

[27] A satellite measurement of reduced planetary albedo may not be able to distinguish between (1) BC in the snow and (2) BC in the atmosphere above the snow ("Arctic haze") [Cess, 1983; Blanchet and List, 1987; Shaw, 1995; Quinn *et al.*, 2007]. Clarke and Noone [1985] estimated that over the Arctic Ocean, the solar energy absorbed by soot in snow was comparable to that absorbed by the Arctic haze. Both will give similar spectral signatures when viewed from above, but their climatic consequences are different: for example, soot in the atmosphere shields the surface from sunlight and stabilizes the atmospheric temperature profile.

9. Greenland

[28] The one region of the Arctic that is unaffected by the snow-thickness ambiguity is the Greenland Ice Sheet. However, its snow has the lowest BC content of the Northern Hemisphere, $C_{BC} \approx 3$ ppb [Doherty *et al.*, 2010]. The fine-grained cold snow near Summit Station should suffer a corresponding albedo reduction of only 0.3% at the most sensitive wavelength [Warren and Wiscombe, 1985, Figure 2], which is unlikely to be reliably detected in a radiation measurement. Attribution would also be difficult because of the depth-gradient of grain size within the top meter.

[29] In the percolation zone and the wet-snow zone of the Greenland Ice Sheet, the BC is largely left behind at the surface as the snow melts, so that during July its mixing ratio in the top few centimeters can rise to 10–20 ppb [Doherty *et al.*, 2010, Figure 10a, Table 6]. The grain size of melting

snow is also larger, allowing the albedo reduction in the mid-visible to reach 3–4%, which might be detectable remotely.

10. Heavily Polluted Snow in Middle Latitudes

[30] Midlatitude snow has higher BC deposition rates but also higher snowfall rates, so the BC mixing ratio is often no greater than in the Arctic, for example in Washington State, Texas, and Nova Scotia [Flanner *et al.*, 2007, Table 2]. However, some regions are polluted sufficiently to cause large albedo reductions, e.g., in northeast China [Huang *et al.*, 2010]. Indeed, some highly contaminated snow in a large city in Japan, with concentrations 2–3 orders of magnitude larger than those of Arctic snow, was apparently quantifiable in a radiation measurement [Kuchiki *et al.*, 2009]. But remote sensing of BC in snow would be difficult even in highly polluted regions of Japan and China because much of the area is forested. There are nonforested parts of these regions (farmland and lakes) where remote sensing of LAI may be possible and could be useful for agricultural and hydrological forecasts, even though these areas are too small to affect global climate.

[31] In the mountainous terrain of the Himalaya, the small scale of the glaciers, their variable and sometimes steep slopes, and the surface features (crevasses, glacial debris) provide obstacles to remote retrieval of impurity concentrations in snow. Here the major LAI is apparently dust rather than BC. Painter *et al.* [2012] used MODIS to infer radiative forcing by dust contamination of snow in the Himalaya and in southwest Colorado; they made ground-truth measurements in Colorado. The snow was grossly contaminated, with concentrations in the parts-per-thousand range rather than parts per billion. The MODIS retrieval found an astonishingly large mean dust-in-snow forcing of ~ 250 W m⁻² in these regions. Without additional information, this method probably cannot distinguish between dusty snow and dust in the atmosphere above the snow in snapshots, but they might be distinguished in time series. The rms error of the forcing, 32 W m⁻², is smaller than the huge dust-in-snow forcing in Colorado and the Himalaya, but this error is an order of magnitude larger than the forcings expected in more lightly polluted regions such as the Arctic.

[32] Zege *et al.* [2011] have developed a method to infer snow grain size and BC content simultaneously from MODIS. Assuming grain size constant with depth, they concluded that BC in snow can be estimated to 10% accuracy for $C_{BC} = 1000$ ppb, and that for $C_{BC} = 100$ ppb the uncertainty is a factor of 2. They recommend the use of their algorithm only for $C_{BC} \geq 1000$ ppb, effectively limiting its use to highly polluted snow near industrial cities.

11. Summary

[33] The amounts of BC found in Arctic and subarctic snow, as well as in much of the midlatitude snow, are typically 3–30 ppb by mass, sufficient to reduce visible snow albedo by at most a few percent, depending on snow grain size. These reductions can be significant for climate, but direct measurement and attribution of the small signal are difficult. Remote sensing is not likely to be useful for quantifying the effect of BC on snow albedo, because of surface roughness, thin clouds, and especially snow

thinness and patchiness. Each of these conditions can change remotely inferred surface albedo by several percent, comparable to the albedo change from expected BC concentrations in surface snow, thereby confounding the attribution of detected albedo changes. The problems of snow thinness and patchiness are nonexistent on the Greenland Ice Sheet, where the snow surface is horizontal, uniform, deep, and unvegetated. The most favorable location for remote sensing would be the wet snow zone of Greenland late in the melting season, when BC has become concentrated at the surface. But even this elevated BC mixing ratio is an order of magnitude lower than the lower limit suggested by Zege *et al.* [2011] for remote sensing of BC, even when a factor-of-2 error in retrieved BC mixing ratio is tolerated.

[34] Therefore, in almost all geographical regions of interest for climate, there seems no better way to continue to monitor and study the influence of BC in snow than to continue improving the methods of analyzing snow samples by chemical and filter techniques and to find ways to automate them. With that approach the albedo reduction is not directly measured, so it must be computed by radiative transfer modeling. The modeling therefore must in turn be verified; a promising means of verification uses spectral albedo measurement in controlled experiments on artificial snowpacks with large uniform BC amounts [Brandt *et al.*, 2011; Hadley and Kirchstetter, 2012].

[35] **Acknowledgments.** Discussions with Richard Brandt, Thomas Grenfell, and Sarah Doherty have helped to clarify this presentation. Figure 1 was drafted by Richard Brandt. Ron Welch provided the original for Figure 2. Three anonymous reviewers provided helpful comments. The research was supported by NSF grant AGS-11-18460.

References

- Armstrong, T., B. Roberts, and C. Swithinbank (1973), Illustrated Glossary of Snow and Ice, 60 pp., Scott Pol. Res. Inst., Cambridge, UK.
- Barrow, G. M. (1962), Introduction to Molecular Spectroscopy, McGraw-Hill, New York.
- Blanchet, J.-P., and R. List (1987), On radiative effects of anthropogenic aerosol components in Arctic haze and snow, *Tellus Ser. B*, *39*, 293–317.
- Brandt, R. E., S. G. Warren, and A. D. Clarke (2011), A controlled snowmaking experiment testing the relation between black carbon content and reduction of snow albedo, *J. Geophys. Res.*, *116*, D08109, doi: 10.1029/2010JD015330.
- Carroll, J. J., and B. W. Fitch (1981), Dependence of snow albedos on solar elevation and cloudiness at the south pole, *J. Geophys. Res.*, *86*, 5271–5276.
- Cess, R. D. (1983), Arctic aerosols: Model estimates of interactive influences upon the surface-atmosphere clear-sky radiation budget, *Atmos. Environ.*, *17*, 2555–2564.
- Clarke, A. D., and K. J. Noone (1985), Soot in the Arctic snowpack: A cause for perturbations in radiative transfer, *Atmos. Environ.*, *19*, 2045–2053.
- Doherty, S. J., S. G. Warren, T. C. Grenfell, A. D. Clarke, and R. E. Brandt (2010), Light-absorbing impurities in Arctic snow, *Atmos. Chem. Phys.*, *10*, 11,647–11,680.
- Flanner, M. G., and C. S. Zender (2005), Snowpack radiative heating: Influence on Tibetan Plateau climate, *Geophys. Res. Lett.*, *32*, L06501, doi: 10.1029/2004GL022076.
- Flanner, M. G., C. S. Zender, J. T. Randerson, and P. J. Rasch (2007), Present-day climate forcing and response from black carbon in snow, *J. Geophys. Res.*, *112*, D11202, doi: 10.1029/2006JD008003.
- Forsström, S., J. Ström, C. A. Pedersen, E. Isaksson, and S. Gerland (2009), Elemental carbon distribution in Svalbard snow, *J. Geophys. Res.*, *114*, D19112, doi: 10.1029/2008JD011480.
- Gow, A. J. (1965), On the accumulation and seasonal stratification of snow at the South Pole, *J. Glaciol.*, *5*, 467–477.
- Grenfell, T. C. (2011), Albedo, in *Encyclopedia of Snow, Ice and Glaciers*, edited by V. P. Singh, P. Singh, and U. K. Haritashya, pp. 23–34, Springer, Dordrecht, Netherlands.
- Grenfell, T. C., and S. G. Warren (1999), Representation of a nonspherical ice particle by a collection of independent spheres for scattering and absorption of radiation, *J. Geophys. Res.*, *104*, 31,697–31,709.
- Grenfell, T. C., S. G. Warren, and P. C. Mullen (1994), Reflection of solar radiation by the Antarctic snow surface at ultraviolet, visible, and near-infrared wavelengths, *J. Geophys. Res.*, *99*, 18,669–18,684.
- Grenfell, T. C., S. J. Doherty, A. D. Clarke, and S. G. Warren (2011), Spectrophotometric determination of absorptive impurities in snow, *Appl. Opt.*, *50*, 2037–2048.
- Greuell, W., and J. Oerlemans (2005), Validation of AVHRR- and MODIS-derived albedos of snow and ice surfaces by means of helicopter measurements, *J. Glaciol.*, *51*, 37–48.
- Greuell, W., C. H. Reijmer, and J. Oerlemans (2002), Narrowband-to-broadband albedo conversion for glacier ice and snow based on aircraft and near-surface measurements, *Remote Sens. Environ.*, *82*, 48–63.
- Hadley, O. L., and T. W. Kirchstetter (2012), Black-carbon reduction of snow albedo, *Nature Clim Change*, *2*, 437–440.
- Hansen, J., and L. Nazarenko (2004), Soot climate forcing via snow and ice albedos, *Proc. Natl. Acad. Sci. USA*, *101*, 423–428.
- Hansen, J., et al. (2005), Efficacy of climate forcings, *J. Geophys. Res.*, *110*, D18104, doi: 10.1029/2005JD005776.
- Huang, J., Q. Fu, W. Zhang, X. Wang, R. Zhang, H. Ye, and S. Warren (2011), Dust and black carbon in seasonal snow across northern China, *Bull. Am. Meteorol. Soc.*, *92*, 175–181.
- Hudson, S. R., and S. G. Warren (2007), An explanation for the effect of clouds over snow on the top-of-atmosphere bidirectional reflectance, *J. Geophys. Res.*, *112*, D19202, doi: 10.1029/2007JD008541.
- Hudson, S. R., S. G. Warren, R. E. Brandt, T. C. Grenfell, and D. Six (2006), Spectral bidirectional reflectance of Antarctic snow: Measurements and parameterization, *J. Geophys. Res.*, *111*, D18106, doi: 10.1029/2006JD007290.
- Kuchiki, K., T. Aoki, T. Tanikawa, and Y. Kodama (2009), Retrieval of snow physical parameters using a ground-based spectral radiometer, *Appl. Opt.*, *48*, 5567–5582.
- Kuhn, M. (1974), Anisotropic reflection from sastrugi fields, *Antarctic J. U. S.*, *9*(4), 123–125.
- LaChapelle, E. R. (1969), Field Guide to Snow Crystals, Univ. of Wash., Seattle, Wash.
- Leroux, C., and M. Fily (1998), Modeling the effect of sastrugi on snow reflectance, *J. Geophys. Res.*, *103*(E11), 25,779–25,788.
- Masonis, S. J., and S. G. Warren (2001), Gain of the AVHRR visible channel as tracked using bidirectional reflectance of Antarctic and Greenland snow, *Int. J. Remote Sensing*, *22*, 1495–1520.
- Matzl, M., and M. Schneebeli (2006), Measuring specific surface area of snow by near-infrared photography, *J. Glaciol.*, *52*, 558–564.
- Matzl, M., and M. Schneebeli (2010), Stereological measurement of the specific surface area of seasonal snow types: Comparison to other methods, and implications for mm-scale vertical profiling, *Cold Regions Sci. Technol.*, *64*, 1–8.
- McConnell, J. R., R. Edwards, G. L. Kok, M. G. Flanner, C. S. Zender, E. S. Saltzman, J. R. Banta, D. R. Pasteris, M. M. Carter, and J. D. W. Kahl (2007), 20th century industrial black carbon emissions altered Arctic climate forcing, *Science*, *317*, 1381–1384, doi: 10.1126/science.1144856.
- Nolin, A. W., and J. Dozier (2000), A hyperspectral method for remotely sensing the grain size of snow, *Remote Sens. Environ.*, *74*(92), 207–216.
- O’Rawe, P. (1991), Monte Carlo Models for the Reflection of Sunlight from Rough Snow Surfaces: Suncups and Sastrugi, M.S. thesis, 521 pp., Univ. of Wash., Seattle, Wash.
- Painter, T. H., A. C. Bryant, and S. M. Skiles (2012), Radiative forcing by light absorbing impurities in snow from MODIS surface reflectance data, *Geophys. Res. Lett.*, *39*, L17502, doi: 10.1029/2012GL052457.
- Post, A., and E. R. LaChapelle (2000), *Glacier Ice*, 145 pp, Univ. of Wash., Seattle, Wash.
- Qian, Y., M. G. Flanner, L. R. Leung, and W. Wang (2011), Sensitivity studies on the impacts of Tibetan Plateau snowpack pollution on the Asian hydrological cycle and monsoon climate, *Atmos. Chem. Phys.*, *11*, 1929–1948.
- Quinn, P. K., G. Shaw, E. Andrews, E. G. Dutton, T. Ruoho-Airola, and S. L. Gong (2007), Arctic haze: Current trends and knowledge gaps, *Tellus Ser. B*, *59*, 99–114.
- Rhodes, J. J., R. L. Armstrong and S. G. Warren (1987), Mode of formation of “ablation hollows” controlled by dirt content of snow, *J. Glaciol.*, *33*, 135–139.
- Shaw, G. E. (1995), The Arctic haze phenomenon, *Bull. Am. Meteorol. Soc.*, *76*, 2403–2413.
- Stroeve, J., J. E. Box, C. Fowler, T. Haran, and J. Key (2001), Intercomparison between in-situ and AVHRR Polar Pathfinder-derived surface albedo over Greenland, *Remote Sens. Environ.*, *75*, 360–374.

WARREN: REMOTE SENSING OF BC IN SNOW

- Suttles, J. T., R. N. Green, P. Minnis, G. L. Smith, W. F. Staylor, B. A. Wielicki, I. J. Walker, D. F. Young, V. R. Taylor, and L. L. Stowe (1988), Angular Radiation Models for Earth-Atmosphere System, vol. 1, . Shortwave Radiation, NASA Ref. Publ. 1184.
- Twohy, C. H., A.D. Clarke, S. G. Warren, L. F. Radke and R. J. Charlson (1989), Light-absorbing material extracted from cloud droplets and its effect on cloud albedo, *J. Geophys. Res.*, *94*, 8623–8631.
- Warren, S. G. (1982), Optical properties of snow, 1982, *Rev. Geophys. Space Phys.*, *20*, 67–89.
- Warren, S. G. and R. E. Brandt (2008), Optical constants of ice from the ultraviolet to the microwave: A revised compilation, *J. Geophys. Res.*, *113*, D14220, doi: 10.1029/2007JD009744.
- Warren, S. G., and A. D. Clarke (1990), Soot in the atmosphere and snow surface of Antarctica, *J. Geophys. Res.*, *95*, 1811–1816.
- Warren, S.G., and W.J. Wiscombe (1980), A model for the spectral albedo of snow. II: Snow containing atmospheric aerosols, *J. Atmos. Sci.*, *37*, 2734–2745.
- Warren, S. G., and W. J. Wiscombe (1985), Dirty snow after nuclear war, *Nature*, *313*, 467–470.
- Warren, S. G., I. G. Rigor, N. Untersteiner, V. F. Radionov, N. N. Bryazgin, Y. I. Aleksandrov, and R. Colony (1999), Snow depth on Arctic sea ice, *J. Clim.*, *12*, 1814–1829.
- Warren, S. G., R. E. Brandt, and P. O’Rawe Hinton (1998), Effect of surface roughness on bidirectional reflectance of Antarctic snow, *J. Geophys. Res.*, *103*, 25,789–25,807.
- Welch, R. M., and B. A. Wielicki (1989), Reflected fluxes for broken clouds over a Lambertian surface, *J. Atmos. Sci.*, *46*(10), 1384–1395.
- Wiscombe, W. J., and S. G. Warren (1980), A model for the spectral albedo of snow, I: Pure snow, *J. Atmos. Sci.*, *37*, 2712–2733.
- Zege, E. P., I. L. Katsev, A. V. Malinka, A. S. Prikhach, G. Heygster, and H. Wiebe (2011), Algorithm for retrieval of the effective snow grain size and pollution amount from satellite measurements, *Rem. Sens. Environ.*, *115*, 2674–2685.